Hydrol. Earth Syst. Sci. Discuss., 8, 11039–11073, 2011
www.hydrol-earth-syst-sci-discuss.net/8/11039/2011/
doi:10.5194/hessd-8-11039-2011


Hydrology and Earth System Sciences Discussions







# A conceptual model of the hydrological influence of fissures on landslide activity

**D. M. Krzeminska[1], T. A. Bogaard[1], Th. W. J. van Asch[2], and L. P. H. van Beek[2]**

[1]Delft University of Technology, Water Resources Section, P.O. Box 5048, 2600 GA Delft, The Netherlands
[2]Utrecht University, Faculty of Geosciences, UCEL P.O. Box 80115, 3508 TC, Utrecht, The Netherlands

Received: 24 November 2011 – Accepted: 6 December 2011 – Published: 13 December 2011

Correspondence to: D. M. Krzeminska (d.m.krzeminska@tudelft.nl)

Published by Copernicus Publications on behalf of the European Geosciences Union.

## Abstract

Hydrological processes control the behaviour of many unstable slopes and their importance for landslide activity is generally accepted. In slow-moving landslides differential displacement complicates the hydrological regime due to continuous opening and closing of the fissures and cracks, creating dynamic preferential flow path systems. The consequences of the appearance and destruction of these preferential flow paths is thus closely related to the formation of critical pore pressure and the resulting movement and persistence of fissure systems. This interaction may account for the seasonal nature of the slow-moving landslide activity, including the often observed shifts and delays.

This research aims to investigate this interaction between slope stability and spatial and temporal variations in fissure patterns, which makes fissures act both as preferential flow paths for infiltration and as lateral groundwater drains. To this end, the hydrological processes that control exchange of water between the fissure network and the matrix has been included in a spatially distributed hydrological and slope stability model. The ensuing feedbacks in landslide activity were explored by running the model with the meteorological forcing of one year until a dynamic steady-state was achieved. The effect of fissure dynamics was evaluated by comparing simulations with static fissure patterns to those in which these patterns deform as function of the local stability.

## 1 Introduction

### 1.1 Motivation and objective

Hydrology has long been recognized as a crucial factor in initiation and reactivation of landslides. The internal strength of the slope is decreases as the groundwater level rises and pore pressure increases. However, precipitation itself has limited predictive value for activity of slow-moving landslide (Bogaard and Van Asch, 2002; Van Asch et al., 2007) and the timing, intensity and the duration of mass movement is not always directly correlated with the timing and intensity of the rainfall (Malet et al., 2002). The unsaturated zone controls groundwater recharge allowing for the loss of soil moisture by evaporation, attenuating the percolation and providing preferential flow paths (formed by soil fauna, by plant roots, soil erosion, etc; Beven and Germann, 1982) for infiltrating water (Bogaard, 2001; Krzeminska et al., 2011). Additionally, in slow-moving landslide, constant movement of the sliding material results in fissure formation due to compression and extension. This creates dual permeability networks with dynamically changing hydraulic properties of the secondary porosity that influence the time and intensity of groundwater recharge.

The distribution of fissures and their hydrological characteristics within a slow-moving landslide can change due to displacement or changes in the stress field (Bogaard, 2001; Van Asch et al., 2001). For the purpose of this study we will use the term ‘fissures’ to refer to geo-mechanically induced cracks that are filled or partly filled with reworked material. Based on the double-porosity theory (Barenblatt et al., 1960) appearance of fissures creates a system consisting of two media: the fractures and the matrix blocks, both of them having their own characteristic properties (i.e. porosity, hydraulic conductivity). However, the double-porosity approach assumes that water flow is confined to the fissure domain (mobile-immobile-type of transport). Therefore, we use the dual-permeability approach which is an extension of the double-porosity approach by allowing water flow in both domains (matrix and fissures). Accordingly, we use the term “preferential fissure flow” to refer to rapid water flow in fissure bypassing the bulk flow of the less pervious matrix (Beven and Germann, 1982). These fissures can act both as preferential flow paths for infiltration and as lateral groundwater drains. As such, they have strong influence on groundwater level fluctuation, and thus, on slope stability.

The main goal of this research is to study the importance of preferential fissure flow for landslide hydrological behaviour and slope stability at the field scale. The



HESSD
8, 11039–11073, 2011
Influence of fissures on landslide activity
D. M. Krzeminska et al.

conceptual model was based on the Storage and Redistribution of Water on Agricultural and Re-vegetated Slopes model (STARWARS), which is a distributed model coupling hydrological and stability dynamics (Van Beek, 2002).

### 1.2 Preferential fissure flow in landslide

Macropores are defined as structural pores of large diameter (minimum 30–3000 µm; Beven and Germann, 1982) that drain mainly by gravitational forces (laminar water flow, not influenced by capillarity). Fissures are a special case of macropores with apertures that vary from few up to tens of centimetres. The importance of macropore flow for slope hydrology (including slope stability) was recognised in early 1980s (Pierson, 1983; Brand et al., 1986) and since then has been receiving lot of research attention (Tsuboyama et al., 1994; Noguchi et al., 1999; Nobles et al., 2004; Nieber and Sidle, 2004).

Various authors reported adverse and beneficial effects on macropore flow (including fissure flow) on landslide activity (McDonnell, 1990; Van Beek and Van Asch, 1999; Fannin et al., 2000; Uchida et al., 2001). Presence of fissures can lead to slope instability by influencing storage capacity of the soil and affects the infiltration processes of rainfall. Fast flow through the fissures may increase the rate of vertical infiltration providing direct access to the lower groundwater and increasing the rate of groundwater recharge. On the other hand an extended fissures network may increase the rate of natural soil drainage, which limits the building up of water pressure. However, when talking about dead-end fissures (disconnected fissure network), once their storage capacity is exceeded, they contribute to maintain high pore water pressures in the surrounding soils (McDonnell, 1990; Van Asch et al., 1996; Uchida et al., 2001).

Initiation of macropore flow depends mainly on antecedent soil moisture content, rainfall amount and intensity, hydraulic conductivity of the soil matrix, density and distribution of macropores and soil texture (Bouma, 1990; Trojan et al., 1992; Weiler et al., 2003). The macropore flow can be initiated either at the soil surface, when the rainfall intensity exceeds the infiltration rate of the soil matrix, or from a saturated or partially saturated soil layer, when rainfall amount exceeds the saturation deficit of the soil layer. Flow in macropores can occur with or without interaction with the surrounding soil-matrix, depending on soil matrix properties and soil water content, properties of macropores and matrix-macropore interface. Water can flow into a macropore if its water entry pressure is exceeded, either at the soil surface or the nearly saturated subsurface (Weiler et al., 2003).

The effectiveness of macropores (fissures) for transmitting water downslope depends upon their size, spatial distribution, and connectivity (Beven and Germann, 1982; McDonnell, 1990; Cameira et al., 2000; Nobles et al., 2004). The larger macropores are, the more water they can potentially conduct or store, depending on the connectivity between macropores. The macropores themselves are not considered to be continuous throughout the soil profile or the hillslope but more likely they are separated by the matrix blocks located at the endpoints of the individual macropores (e.g. Noguchi et al., 1999; Sidle et al., 2001). In this way, the macropores connectivity depends on water content in separating matrix blocks and the degree of macropore effectiveness increase with wetness (Tsuboyama et al., 1994; Sidle et al., 2000). However, despite field evidence, laboratory experiments and analytical research, the relationship between soil moisture and macropore connectivity is qualitative only (Nieber and Sidle, 2004) and its quantification remains difficult.

The complexity of the preferential flow processes and their high spatial and temporal variability make it very difficult to measure the processes in the field and to upscale the information to the catchment scale (Van Schaik, 2010). In slow-moving landslide constant movement of the sliding material and its heterogeneity makes the preferential fissure flow paths system difficult to characterise. Moreover, constant opening and closing of the aperture in the reworking material makes it even more difficult to monitor and to model.





HESSD
8, 11039–11073, 2011

## 1.3 Hydrological modelling of rainfall induced landslide

To analyse rainfall induced landsliding, governed by either unsaturated or saturated conditions, several models were propose (Wu and Sidle, 1995; Van Beek and Van Asch, 1999; Iverson, 2000; Brooks et al., 2002; Cappa et al., 2004). Numerical codes vary from simple 1-D lumped models to complex physically based 3-D models and can involve either traditional (area-average values of equivalent parameters) or distributed approaches. Distributed approaches are the most suitable to account for spatial and temporal heterogeneity of the hydrological systems (e.g. Miller and Sias, 1998) and thus, they improve forecasting of spatio-temporal probabilities of landslide (Van Westen et al., 2005; Malet et al., 2005).

Incorporating preferential flow modelling into a hillslope scale hydrological model is difficult due to the complexity of the phenomena. At the field scale, the majority of macropore flow models use deterministic methods to study water transport (Van Schaik, 2010) and preferential flow is often modelled indirectly as a simplified system with preferential vertical fluxes (Bogaard, 2002) or rapid slope-parallel flow on the bedrock surface without taking into account the distributed nature of the soil macropores system (Beckers et al., 2004; Kosugi et al., 2004). Moreover, in many large scale models, preferential flow is included as a modification of hydraulic conductivity function (e.g. Mulungu et al., 2005; Zhang et al., 2006). Zehe and Bloschl (2004) used a threshold function to switch on macropores flow and established a linear increase of the hydraulic conductivity with increasing relative saturation of the soil for both plot and catchment scale hydrological modelling.

Weiler et al. (2007) stressed that conceptualization and parameterization of the effect of lateral preferential flow on hillslope hydrology is one of the great challenges. They attempt to combine the quantitative and qualitative approach to incorporate the spatially dynamic nature of preferential flow system by bringing lateral preferential flow into a formal model structure as randomly generated pipe network.





HESSD
8, 11039–11073, 2011

## 1.4 The hydrological model STARWARS

In 1999, Van Beek and Van Asch proposed conceptual hillslope model that account for fissure-induced infiltration. This is spatially distributed physically based model coupling hydrological and stability dynamics in the PCRaster environmental modelling software package. Subsequently, Van Beek (2002) developed the STARWARS model that consists of a core model resolving dynamic equation of saturated and unsaturated flow and of sub-models that describe specific hydrological process such us interception, transpiration, snow cover or snow melt (Fig. 1; Van Beek, 2002). The use of meta-language of PCRaster GIS package provides an expedient way to include and change spatially distributed hydrological and geotechnical parameters.

The model represents the soil mantle (as a column of three layers) overlying a semi-impervious bedrock. The layers have variable depth centred on the mid-point or node of each cell of an equidistant grid in the x- and y-direction (Van Beek, 2002). The hydrological model describes the saturated ($Q_{\mathrm{sat}}$) and the unsaturated ($Pe$) transient flow in the vertical and horizontal direction assuming freely drainable water (unconfined groundwater levels). Precipitation ($P$) and evaporation ($E$) constitute the boundary condition at the top of the soil column. The percolation loss across the lithic contact into the underlying bedrock reservoir constitutes the lower boundary condition (BC). It accounts for macropore or fissure flow in a rather simplistic way, by allowing a fraction of the surface detention to bypass the unsaturated matrix and recharge the groundwater table directly (Fig. 2a). For a complete description of the model the reader is refered to Van Beek (2002).

Since its development, the STARWARS model has been used by many researchers to study different hydrological and ecological issues for both synthetic and real case studies (Van Beek, 2002; Malet et al., 2005; Kuriakose et al., 2009; Brolsma, 2010). In 2005, Malet et al. applied the STARWARS model to the Super-Sauze landslide using the simple bypass flow scheme: only shallow bypassing flow without fissure - matrix interaction (Fig. 2a). Malet et al. (2005) concluded that accounting for fissure flow was





HESSD
8, 11039–11073, 2011

an important improvement in modelling the hydrology of the landslide and stressed a need for further specific research on this topic.

Here, we adapted the STARWARS model by introducing a conceptual fissure flow routine to represent shallow bypass flow in an expedient way. The fissure network consists of a set of near-vertical open voids which is introduced by disaggregating the cell volumes into soil matrix volume and fissures volume. This fissure network is described by two parameters: an average volumetric fraction of soil occupied by fissures or macropores and a mean effective fissure aperture. Interaction between the matrix and fissure network is taken into account and depends on the water level in the fissure and height of the perched water table in the matrix: saturated outflow from the matrix and water infiltration from the fissure to the matrix over both the saturated and unsaturated zone of contact between them.

As stated before (Sect. 1.2) fissure connectivity and density are one of the most important characteristics determining the influence of fissures on landslide hydrology. In order to mimic dynamic feedback between fissures characteristics, slope stability and hydrology we established two relationships: a dependency of fissure connectivity upon relative degree of saturation of the matrix and a relationship between potential movement of the landslide and density of the fissure network. Herein we focus on first relationship, which is already getting research attention.

## 2 Adaptation of STRAWARS – concept of fissure representation

The inclusion of fissures in STARWARS required an adaptation of the existing model concept (Fig. 2b). The new concept assumes (after Van Beek and Van Asch, 1999) that fissures are distinct from the matrix and are represented within each cell as a continuous network of highly pervious zones surrounded by matrix blocks. For each layer of the soil column the fissure distribution is prescribe by the fractional area covered by fissure ($F_{\mathrm{fis}}$) and mean fissure aperture ($a_{\mathrm{fis}}$[m]). They are distributed evenly throughout the cell and they extend vertically over the full depth of the layer. Fissures can be filled or partly filled with reworking material, and thus they have their own porosity. They also maintain their own water level and soil moisture content. Connectivity between the fissure networks in adjacent cells is prescribed fractionally in the x- and y-directions. It is important to keep in mind that fissures characteristics, as all input parameters in the model, can be spatially differentiated.

The number of fissures per cell ($N_{fis}$) is calculated as:

$$N_{fis} = \sqrt{F_{fis}} \frac{\Delta x}{a_{fis}} \tag{1}$$

where $\Delta x$ is the cell length [m]. $N_{fis}$ is rounded down to the nearest whole number with a minimum value of 1 if $a_{fis} > 0$. In that case, the fractional area covered by fissures is reset to the area of $(2a_{fis}\Delta x - a_{fis}^2)/\Delta x^2$. The spacing of fissures equals the length of the matrix blocks. As it is assumed that in a block all fissures are contained by matrix, there are $N_{fis} + 1$ matrix blocks of width $L_{mat}$ [m]:

$$L_{mat} = \left(1 - \sqrt{F_{fis}}\right) \cdot \frac{\Delta x}{N_{fis} + 1} \tag{2}$$

The approximate mean distance from the centre of a fissure to the centre of each matrix block that defines the different gradients is consequently given by:

$$\overline{\frac{1}{2} L_{mat}} = \frac{2L_{mat} + \frac{1}{2}(N_{fis} - 1)L_{mat}}{N_{fis} + 1} \tag{3}$$

Following the original process description of the STARWARS model (Van Beek, 2002), the unsaturated flow, both in matrix and fissures, is gravitational and vertical only. Percolation is passed on vertically between the layers of the soil column. When the percolation flux in the lowest layer exceeds the basal loss a groundwater table is formed and it rise upward with the assumption that it is vertically contiguous (for both, matrix and fissures fraction). Surface fluxes (infiltration and evaporation) are partitioned on the basis of the respective surface area $A$[m$^2$] calculated as $A_{fis} = F_{fis}\Delta x^2$ for fissure





HESSD
8, 11039–11073, 2011

fraction and $A_{mat} = 1 - A_{fis}$ for matrix fraction. The infiltration capacity of the fissure fraction network is potential unlimited. Fissures can be recharged directly by rain or snow melt or indirectly by overland flow. Moreover, any water that cannot infiltrate into the matrix is passed on to the fissure network.

The storage capacity of a single cell is the combination of matrix and fissure fraction capacity. Fissures maintain their own moisture content and water tables. Any water in excess of the storage capacity of the particular layer is passed on to the overlying layer and any water in excess of the total storage capacity of the matrix within a particular soil column is passed on to saturated storage in the fissure network. When the amount of water exceeds the total available storage capacity of the fissure network within the cell, overland flow occurs. Any water remaining as surface detention is redistributed instantaneously as overland flow over the slope.

Lateral exchange $\Gamma$ [$m^3 h^{-1}$] within the cell is possible only between the saturated zones of matrix and fissure fractions ($\Gamma_{Sat,FM/MF}$) and the unsaturated zones of the matrix fraction and the saturated zone of the fissure fraction ($\Gamma_{Unsat,FM}$) when water level in the fissure fraction exceeds that in the matrix fraction. No lateral fluxes occur between the unsaturated zone of fissure network and unsaturated matrix. However, fissures can drain vertically into the soil when they terminate above the lithic contact. Lateral flow ($Q_{sat}$) between the cells occurs across the saturated zone as result of differences in total piezometric head in the matrix and fissure network between the adjacent nodes in the x- and y-direction. There is no explicit "fissure to fissure in adjacent cell" exchange of groundwater. The total saturated lateral flux is subsequently divided over the matrix and fissure network on the basis of the difference in the local transmissivity which is weighted depending on the connectivity of the fissure network.

Within each model run all the calculation of particular processes within each soil column is ordered as follows: reading the initial conditions (water level and soil moisture content in the matrix and in the fissures), evaluating upper and lower boundary condition, calculation of vertical fluxes, updating the storage capacities, evaluation of lateral fluxes and updating the storage capacities which set new initial conditions for





HESSD
8, 11039–11073, 2011

next step. Although each soil column has a certain storage volume to accommodate the unsaturated and saturated fluxes, all fluxes are calculated at and between nodes.

At the end of each model run factor of safety ($f_s$) is calculated as the ratio between maximum shearing resistance to failure and shear stress:

$$f_s = \frac{c + (\sigma - u)\tan\phi}{\frac{W_{fis}+W_{mat}}{\Delta x^2}\sin\beta\cos\beta} \quad (4)$$

where $c$ is cohesion, $\sigma$ is total normal stress, $u$ is pore pressure and $\phi$ is the angle of internal friction. $W_{fis}$ and $W_{mat}$ are the weight of the fissure and matrix fraction of the cell and $\beta$ is the slope angle.

The infinite slope model is used to calculated slope stability (Milledge et al., 2011). The interaction between cells is neglected and the calculated stability is dependent on the local cell attributes only. The model uses the soil mantle schematisation shown in Fig. 2b with fixed depth equal the depth of the third layer and the lithic contact is assumed to be the potential shear surface. In this way $f_s$ serves here as a proxy for the excess shear stress that cannot be accommodated by a particular soil column.

## 3 Methodology

### 3.1 "Simple" landside representation

Model development and evaluation of the proof-of-concept are carried out using an idealised landslide representation. The idealised digital elevation model (DEM) extends between 1725 m a.s.l. (toe of the landslide) and 2135 m a.s.l. (crown of the landslide) with the grid size of 5 × 5 m. This corresponds to a planar slope of 25.1 °.

The landslide body is delineated by an ellipse with a length of 800 m and a breadth of 90 m. This allows us to account for the converging and diverging topography effect. The depth of the slip plane along the major slope-parallel-axis of the ellipse is described by the arc of a circle passing through the crown and toe of the landslide body and its





HESSD
8, 11039–11073, 2011

mid-point on the vertical through the centre of the landslide. The maximum depth of the landslide is set to 8 m and it decreases towards the borders (Fig. 3a).

The soil parameters of each layer are set arbitrary based on personal experience in landslide field observation. Figure 3b shows the example of the distribution of soil parameters with depth for matrix and fissure fractions. The saturated hydraulic conductivity ($K_{sat}$) was set to $4.1 \cdot 10^{-5}$, $2.8 \cdot 10^{-5}$ and $2.4 \cdot 10^{-5}$ m s$^{-1}$ for the matrix fraction, for layer 1, 2, and 3 respectively. For each layer, the $K_{sat}$ for fissure fraction was assumed to be 10 times higher than that of the matrix.

### 3.2 Dynamic characteristics of fissure network

Although field studies have shown that the macropore continuity is dynamic and positively related to increase in water content (e.g. Tsuboyama et al., 1994; Sidle et al., 2000), quantification of this relationship remains difficult. Moreover, there is no research on macropore continuity dedicated particularity to the large macropores as fissures. Therefore, in analogy to macropore flow (e.g. Zehe and Bloschl, 2004), we have assumed an overall positive trend between fissures connectivity ($C_{fis}$) and relative effective saturation of ($\Theta_E$) of the surrounding soil, which can be expressed as follows:

$$C_{\mathrm{fis},i} = \begin{cases} \frac{C_{\mathrm{fis,max}} - C_{\mathrm{fis,min}}}{\Theta_{\mathrm{E,sat}} - \Theta_{\mathrm{E,fc}}} (\Theta_{\mathrm{E},i} - \Theta_{\mathrm{E,fc}}) + C_{\mathrm{fis,min}} & \text{for } \Theta_{\mathrm{E},i} \geq \Theta_{\mathrm{E,fc}} \\ C_{\mathrm{fis,min}} & \text{for} \Theta_{\mathrm{E},i} < \Theta_{\mathrm{E,fc}} \end{cases} \quad (5)$$

where $C_{\mathrm{fis},i}$ and $\Theta_E$ are fissure connectivity [-] and effective saturation of the matrix [-] at time step $i$, $C_{\mathrm{fis,min}}$ and $C_{\mathrm{fis,max}}$ are the minimal and maximal fissures connectivity, set to 0.1 and 0.9 respectively; $\Theta_{\mathrm{E,fc}}$ is effective saturation at the field capacity [-] and $\Theta_{\mathrm{E,sat}} = 1$ (full saturation).

Strictly speaking, the effect of moisture content on fissure connectivity is already conceptualized in the model. Each cell is divided between matrix and fissure network. If $C_{fis} = 0$ there is no direct connection between the fissure fractions of adjacent cells. However, there can be an exchange between the fissure fraction and matrix fraction of one cell and matrix fraction and fissure fraction of another cell. Consequently, fissures are indirectly connected via the matrix and then it is the matrix hydraulic conductivity that controls the fluxes.

Introducing a direct relationship between fissure connectivity and soil moisture (Eq. 5) in the model will have direct effect on the drainage capacity of the fissure network. With $C_{fis} > 0$ a direct exchange of water in the fissure network between adjacent cells is possible. In this case, the water flux is controlled by hydraulic conductivity of fissure network. In this way the effect of natural fissure drainage capacity can be mimicked.

### 3.3 Modelling strategy

Four scenarios are evaluated:

- scenario 1 – no fissure – represents the landslide were no fissures are considered;
- scenarios 2 and 3 – connected and disconnected fissures – were fissures properties are set to be constant over the simulation period, and fissure connectivity ($C_{fis}$) is set to be 10 % or 90 % for disconnected fissures and connected fissures scenario respectively;
- scenario 4 – dynamic connectivity – scenario where the dynamic characteristic of fissures connectivity is applied.

Each model run is performed for one year with the use of the same meteorological forcing (rain intensity, air temperature, incoming short wave radiation and relative humidity). The initial conditions (distributed groundwater level, soil moisture and snow thickness) were determined by spinning up the model with the "no fissure" scenario.

For scenarios 2 and 3 (constant fissures scenarios) equal fissures distribution is assumed over whole landslide. An average fissure fraction was set to be equal $F_{fis,max}$ for each of the soil layer (0.30, 0.20 and 0.05 respectively) and an average fissures





HESSD
8, 11039–11073, 2011

aperture ($a_{\mathrm{fis}}$) was set to be 0.20, 0.10 and 0.05 m for 1st, 2nd and 3rd layer respectively. For scenario 4 (dynamic connectivity scenario) the initial $F_{\mathrm{fis}}$ is equal $F_{\mathrm{fis,max}}$. It is important to stress that in the model the geometry of the landslide remains constant during the simulation period, so no mass displacement is considered. The scenarios have no influence on the mechanical material properties.

The outputs of the simulation were collated with each other in order to see the effect of the introduction of fissure and their connectivity on the hydrological behaviour of the landslide. For this, the water balance components are calculated and compared between the different scenarios.

## 4 Results and discussion

### 4.1 General water balance components of a landslide

Table 1 shows the annual water balance components of four modelled scenarios. The initial conditions of each scenario have the same groundwater levels, soil moisture content, surface detention and snow cover. Consequently, the total storage at the start of simulation period is different for the "no fissure" scenario and the other three scenarios: the same groundwater levels but with different porosities because of introducing the fissure network.

In general, there are only small differences in the water balance. The majority of the input (rain water) leaves the system as evaporation: between 64.7 % of rain volume for the "no fissure" scenario and 65.8 % of the rain volume for the "connected fissure" scenario. The total storage capacity of the entire landslide is decreasing for all but the "disconnected fissure" scenario. The highest difference (more than 3 % of the total volume of rain) is observed for the "connected fissure" scenario. The yearly average total storage observed for "dynamic connectivity" is lower than the one observed for the "connected fissure" scenario (2.2 % difference) and always higher than the one





HESSD
8, 11039–11073, 2011

for "disconnected fissure" (1.2 % difference). Consequently, the "connected fissure" scenario shows the highest total outflow equal 37.7 % of total rain volume, while for "disconnected fissure" it is 35.2 % and for "dynamic connectivity" it is 36.7 %.

Figure 4a shows the variation in total storage in relation to cumulated inflow. The difference in total storage between the "no fissure" scenario and the other three scenarios is the consequence of introducing fissures as fraction of landslide material with higher porosity: the same initial groundwater level and soil moisture content but higher porosity results in higher total storage values. However, when looking at the relative changes in total storage, in regards to initial conditions scenarios, one can see that the dynamics of total storage of "no fissure" and "disconnected fissure" are almost equal (Fig. 4b). The overall behaviour of the system is very similar for all the scenarios with clear consecutive drying and wetting periods. Nevertheless, the total storage of "disconnected fissure" is always the highest and the one of "connected fissure" the lowest. It is interesting to see that when the total storage of the landslide is more than 90 % of maximal available storage (MaxStor), the difference between observed and initial total storages is the same for all of the scenarios.

### 4.2 Spatial and temporal differences in groundwater level

The timing and duration of near saturation is an important aspect for landslide (re-)activation. Figure 5 shows the total amount of days (during the one-year simulation period) with total saturation (groundwater level reaching the soil surface). Clear differences between the scenarios can be seen. The average number of days with saturation is 121, 132, 161 and 122 days per cell for scenarios 1 to 4 respectively. While the average number of days with saturation for "no fissure" and "dynamic connectivity" is almost the same, the spatial distribution of the storage (saturation) is different: much less saturation is observed in the upper part of the landslide when accounting for dynamic connectivity of fissures. The results of the "connected fissures" scenario is strongly affected by pre-defined bedrock topography and converging water flow paths. Faster drainage propagates water downslope and vertically converging flow paths result in accumulation of the water in the lower part of the landslide.

It is interesting to compare the results presented in Fig. 5 with Fig. 6 showing the number of unstable cells ($f_s < 1$) observed per time step. The average number of unstable cells observed with "no fissures" and with "dynamic connectivity" is again quite similar, while the "disconnected fissures" and "connected fissures" scenarios presents two extreme behaviours which is the effect of increase ("disconnected fissures") or decrease ("connected fisures") of soil column weight ($W_{fis}, W_{mat}$) due to different water distribution within the landslide.

Figure 7a shows an example of modelled groundwater levels from toe to crown along the landslide for six days during the one year simulation periods. Figure 8 presents an example of the modelled groundwater level fluctuations for four points located along the landslide profile.

In case of "connected fissures" water entering the fissures network is drained out of the landslide by fissures that provide continuous areas of high transmissivity. The total lateral saturated water flow ($Q_{sat}$), that represents lateral drainage within the landslide system (flow between cells), is approximately three times higher than in case of the "no fissure" scenario and 83 % of this water is flowing through the fissure network. As a consequence, a general decrease of the groundwater level is observed (Figs. 7a and 8b–d). On the contrary, the model configuration with "disconnected fissures" creates areas with very high storage capacities but with slower lateral exchange between cells. In this way, groundwater table remains at a higher level compared to the "no fissures" and "connected fissures" scenarios. The total lateral saturated flow, in case of "disconnected fissure", is one and half times higher comparing to the "no fissure" scenario and approximately 60 % of it is a flow occurring between fissure fraction of one cell and matrix fraction of another cell or between fissure fractions of the cells.

The groundwater level simulated with the "dynamic connectivity" scenario is a combination of the modest fluctuations observed for the "disconnected fissures" scenario and the larger groundwater level fluctuation observed for that of "connected fissures".





HESSD
8, 11039–11073, 2011



Title Page
Abstract Introduction
Conclusions References
Tables Figures
◀◀ ▶▶
◀ ▶
Back Close
Full Screen / Esc
Printer-friendly Version
Interactive Discussion

Fissure connectivity changes in time and space (Fig. 7b) according to the relationship defined with Eq. (5). However, the higher total storage of the landslide is the smaller observed differences in groundwater level are between the scenarios (Fig. 7a).

At the lower part of the landslide (Fig. 8e) the groundwater behaviour depends on parallel flow paths (planar) but also converging flow paths (vertical). The simulation results show that this is especially important if a large volume of water can be transported from upslope via fast flow through well connected fissure system (the "connected fissure" scenario). Therefore, in the lower part of the landslide, the highest groundwater level is observed when the "connected fissure" scenario is implemented.

There are significant differences between the scenarios in timing when the saturation is reached (Fig. 8). The highest groundwater level is observed first for "disconnected fissures", then "no fissures", "dynamic connectivity" and lastly the "connected fissures" scenario. The exception is the lowest part of the landslide (Fig. 8e) where, in case of the "connected fissure" scenario most of the water is accumulated and thus groundwater level is the highest.

When looking at the exchange fluxes between fissure and matrix fraction clear differences between scenarios are visible. The absolute total exchange fluxes between fissure and matrix fractions ($\Gamma_{\mathrm{Sat,FM}} + \Gamma_{\mathrm{Sat,MF}} + \Gamma_{\mathrm{Unsat,FM}}$) for "dynamic connectivity" equal 60 % of the one observed for "connected fissure" and almost 200 % of the one observed for "disconnected fissure". The same relation is observed when comparing unsaturated ($\Gamma_{\mathrm{Unsat,FM}}$) and saturated ($\Gamma_{\mathrm{Sat,FM}} + \Gamma_{\mathrm{Sat,MF}}$) exchange fluxes separately. For all scenarios the saturated exchange fluxes ($\Gamma_{\mathrm{Sat,FM}} + \Gamma_{\mathrm{Sat,MF}}$) are 98 % of total exchange fluxes. However, there are significant differences in flux directions. The ratio between the total amount of water flowing from the fissure fraction into the matrix fraction ($\Gamma_{\mathrm{Sat,FM}}$) and the total amount of water flowing from the matrix fraction into the fissure fraction ($\Gamma_{\mathrm{Sat,MF}}$) are 1, 0.75 and 0.5 for "disconnected fissure", "dynamic connectivity" and "connected fissure" respectively. The results of exchange fluxes analysis show that there are limited differences in piezometric head in matrix and fissure network for "disconnected fissure". They also show that in case of "connected fissure" these





HESSD
8, 11039–11073, 2011



D. M. Krzeminska et al.

differences are getting bigger and that groundwater level in the matrix is in general higher than the one in the fissure. The “dynamic connectivity” scenario is combination of two extreme scenarios.

### 4.3 Sensitivity analysis

In general, the sensitivity analysis of the model is in line with the one presented by Van Beek (2002) and Malet et al. (2005). The porosity ($n_{\text{mat}}$, $n_{\text{fis}}$) and saturated hydraulic conductivity ($K_{\text{sat,mat}}$, $K_{\text{sat,fis}}$) are the parameters with the largest influence on the hydrological model (modelled storage). It is not surprising since those two parameters control the soil moisture percolation with depth, groundwater recharge and saturated lateral flow. Changing these two parameters by adding or subtracting 25 % and 50 % of their absolute values (for both matrix and fissures fractions at one time) results in maximal 10 % (for $n$) or 5 % (for $K_{\text{sat}}$) variation in modelled storage. There is an obvious strong positive relationship between changes in soil porosity (for both matrix and fissures fractions) and both saturated and unsaturated storages. In case of changes in $K_{\text{sat}}$, the average total storage is almost constant but an increase in $K_{\text{sat}}$, results in an increase in unsaturated storage in both fissures and matrix fraction and a decrease in corresponding saturated storages.

A more detailed sensitivity analysis of the fissure fraction parameterisation and fissure connectivity was performed to quantify whether the introduction of dynamic fissure behaviour is relevant or if similar hydrological responses could be obtained with adapted hydraulic parameterisation of the fissure system. Figure 9 shows the results of the sensitivity analyses by plotting the number of days a cell was saturated as function of the hydraulic parameterisation of the fissures ($K_{\text{sat,fis}}$, $n_{\text{fis}}$). The reference plot (the “dynamic connectivity” scenario) is located in upper right corner of the sensitivity matrix. Moving along the x-axis Ksat, fis decreases while moving along y-axis the porosity of fissure fraction ($n_{\text{fis}}$) decreases. The lower left plot represents the situation of only matrix flow as the saturated hydraulic connectivity and porosity of matrix and fissure fractions are the same. Note, however, that this is not similar to the “no fissure” scenario as also the air entry value and shape factor of soil water retention curve are defined separately for the fissure fraction. Figure 9 shows that when decreasing $K_{sat,fis}$ the upper part of the landslide exhibits more saturation meaning the groundwater levels remain higher in the upper part of the landslide area, such as also seen when modelling no fissures. This is due to the reduced drainage capacity of the fissure network. On the other hand, when $n_{fis}$, decreases (getting closer to nmat) there are limited differences in water distribution within the landslide but the percentage of the unstable area decreases as a result of the decreasing total storage capacity of the landslide.

Figure 10a shows the results coming from the reference scenarios with no sensitivity analysis. Figure 10b shows the effect of the influence of a fissure network with different fissure connectivities (from 10 to 90 %) that are set constant over the simulation period. The last panel (Fig. 10c) presents the simulation results for the "connected fissures" scenario with fissure connectivity set to 50 % and 90 % but with different lower saturated hydraulic permeability for the fissure fraction ($K_{sat,fis}$). Figure 10 shows that the results of the simulation using constant fissure connectivity differ clearly from the one performed with dynamic fissure connectivity, despite changes in fissure fraction characteristics: fissure connectivity (Fig. 10b) and fissure hydraulic permeability (Fig. 10c).

Comparing the results of Fig. 10b with the "dynamic connectivity" scenario of Fig. 10a we can see that constant fissure connectivity results in more water in the lower part of the landslide and gives a larger average unstable area for similar average total storage. The effect of the saturated permeability of the fissures (Fig. 10c) is basically the drainage capacity, independent of the connectivity fraction. The latter, however, has strong influence on the percentage instable areas within the landslide body.

The general conclusion that can be drawn from the sensitivity analysis is that the dynamic fissure behaviour cannot be mimicked using effective hydraulic parameterisation of the fissure fraction with constant connectivity. The "dynamic connectivity" scenario seems to be able to accommodate more water in the system causing less instability.





HESSD
8, 11039–11073, 2011

## 5 Conclusions

This research aimed to study the importance of preferential fissure flow for landslide hydrological behaviour and slope stability at the field scale with a conceptual modelling approach using the Storage and Redistribution of Water on Agricultural and Revegetated Slopes model (STARWARS), which is a distributed model coupling hydrological and stability dynamics (Van Beek, 2002). It highlights that fissure connectivity and fissure permeability are important parameters of the fissure network that can change the water distribution within the landslide and influence the timing and the duration of the periods of elevated pore pressure conditions.

When a fissure network consists of disconnected fissures only storage capacity increases but outflow is impeded. This results in persistent high groundwater levels and less spatial variations across the landslide. A connected fissures network shows fast preferential drainage as dominant process and thus results in a lower groundwater level. However, because of downslope converging flow paths resulting from bedrock topography, the accumulation of the water from the upper part of the landslide can lead to very high groundwater level in the lower part of the landslide and negatively affect the stability of the toe of the landslide.

Introducing the dynamic characteristic of fissure connectivity dependent on soil moisture content as earlier proposed for soil pipe networks, results in composite behaviour, spanning the above end members. This range of hydrological responses under dry and wet conditions seems to provide an internal control mechanism on deformation and introduces stronger seasonality then static fissure connectivity, which is more like what is observed in nature. The analyses showed furthermore that dynamic fissure behaviour could not be mimicked using adjusted hydraulic parameterisation for the fissures. We recognize the difficulties in obtaining the dynamic fissure connectivity, but we believe we showed it is worthwhile to include dynamic fissure characteristics into hydrological modelling of the landslide.

Our research indicates the need for further research into direction of measuring and monitoring of fissures characteristic and their variation over time. This would allow to





HESSD
8, 11039–11073, 2011



Title Page
Abstract | Introduction
Conclusions | References
Tables | Figures
◀◀ | ▶▶
◀ | ▶
Back | Close
Full Screen / Esc
Printer-friendly Version
Interactive Discussion

better constrain the proposed relationship between fissure connectivity and soil moisture content, and to define other relationships, i.e. between fissure volume and differential soil movement within a landslide.

*Acknowledgements.* This research is a part of the "Mountain Risks" project which is funded under the Marie Curie Research Training Network programme within the 6th Framework Programme of the European Commission, under Contract No. MRTN-CT-2006-035798 (http://mountain-risks.eu).

## References

Barenblatt, G. I., Zheltov, I. P., and Kochina, I. N.: Basic concepts in the theory of seepage of homogeneous liquids in fissured rocks, J. Appl. Math., 24, 1286–1303, 1960. 11041

Beckers, J. and Alila, Y.: A model of rapid preferential hillslope runoff contributions to peak flow generation in a temperate rain forest watershed, Water Resour. Res., 40, W03501, doi::10.1029/2003WR002582, 2004. 11044

Beven, K. and Germann, P.: Macropores and water flow in soils, Water Resour. Res., 18, 1311–1325, 1982. 11041, 11043

Bogaard, T. A.: Analysis of hydrological processes in unstable clayey slopes, PhD Thesis, University of Utrecht, The Netherlands, 2001. 11041

Bogaard, T. A.: A state-dependent ground water recharge model for landslide research, which simulates preferential flow, in: Proceedings of the 9th International IAEG congress, Durban, South Africa, 16–20 September, 2002 11044

Bogaard, T. A. and van Asch, T. W. J.: The role of the soil moisture balance in the unsaturated zone on movement and stability of the Beline landslide, France, Earth Surf. Proc. Land., 27, 1177–1188, 2002. 11041

Bouma, J.: Using morphometric expressions for macropores to improve soil physical analyses of field soils, Geoderma, 46, 3–11, 1990. 11042

Brand, E. W., Dale, M. J., and Nash, J. M.: Soil pipes and slope stability in Hong Kong, Q. J. Eng. Geol., 19, 301–303, 1986. 11042

Brolsma, R.: Effect of climate change on temperate forest ecosystems, PhD Thesis, University of Utrecht, The Netherlands, 2010. 11045

Brooks, S. M., Crozier, M. J., Preston, N. J., and Anderson, M. G.: Regolith stripping and the control of shallow translational hillslope failure: application of a two-dimensional coupled soil hydrology-slope stability model, Hawke's Bay, New Zealand, Geomorphology, 45, 165–179, 2002. 11044

Cameira, M. R., Ahuja, L., Fernando, R. M., and Pereira, L. S.: Evaluating field-measured soil hydraulic properties in water transport simulations using the RZWQM, J. Hydrol, 236, 78–90, 2000. 11043

Cappa, F., Guglielmi, Y., Merrien-Soukatchoff, V., Mudry, J., Bertrand, C., and Charmoille, A.: Hydromechanical modeling of a large moving rock slope inferred from slope levelling coupled to spring long term hydrochemical monitoring: example of the La Clapi'ere landslide (Southern Alps, France), J. Hydrol., 291, 67–90, 2004. 11044

Fannin, R. J., Jaakkola, J., Wilkinson, J. M. T., and Hetherington, E. D.: Hydrologic response of soils to precipitation at Carnation Creek, British Columbia, Canada, Water Resour. Res., 36, 1481–1494, 2000. 11042

Iverson, R. M.: Landslide triggering by rain infiltration, Water Resour. Res., 36, 1897–1910, 2000. 11044

Kosugi, K., Uchida, T., and Mizuyama, T.: Numerical calculation of soil pipe flow and its effect on water dynamics in a slope, Hydrol. Process., 18, 777–789, 2004. 11044

Krzeminska, D. M., Steele-Dunne, S. C., Rutten, M. M., Bogaard, T. A., and Sailhac, P.: High resolution temperature observations to monitor hydrological features in reworked clay shales slopes, Hydrol. Process., online first, doi:10.1002/hyp.7980, 2011. 11041

Kuriakose, S. L., van Beek, L. P. H., and van Westen, C. J.: Parameterizing a physically based shallow landslide model in a data poor region, Earth Surf. Proc. Land., 34, 867–881, 2009. 11045

Malet, J.-P., Maquaire, O., and Calais, E.: The use of Global Positioning System for the continues monitoring of landslides, Aplication to the Super-Sauze earthflow (southern Alps, France), Earth Surf. Proc. Land., 28, 541–564, 2002. 11041

Malet, J.-P., van Asch, Th. W. J., van Beek, R., and Maquaire, O.: Forecasting the behaviour of complex landslides with a spatially distributed hydrological model, Nat. Hazards Earth Syst. Sci., 5, 71–85, doi:10.5194/nhess-5-71-2005, 2005. 11044, 11045, 11056, 11064, 11065

McDonnell, J. J.: The influence of macropores on debris flow initiation, Q. J. Eng. Geol. Hydrog., 23, 325–331, doi:10.1144/GSL.QJEG.1990.023.04.06, 1990. 11042, 11043

Milledge, D., Griffiths, V., Warburton, J., and Lane, S.: Can we use the infinite slope model within catchment scale landslide models given its landslide length assumption?, Geophysical Research Abstracts, EGU-11 General Assembly, Vienna, Austria, Vol. 13, EGU2011-3127, 2011. 11049

Miller, D. J. and Sias, J.: Deciphering large landslides: linking hydrological groundwater and stability models through GIS, Hydrol. Process., 12, 923–941, 1998. 11044

Millington, R. J. and Quirk, J. P.: Permeability of porus media, Nature, 183, 387–388, 1959.

Mulungu, D. M. M., Ichikawa, Y., and Shiiba, M.: A physically based distributed subsurface-surface flow dynamics model for forested mountainous catchments, Hydrol. Process., 19, 3999–4022, 2005. 11044

Nieber, J. L. and Sidle, R. C.: How do disconnected macropores in sloping soils facilitate preferential flow, Hydrol. Process., 24, 1582–1594, doi:10.1002/hyp.7633, 2010 11042, 11043

Nobles, M. M., Wilding, L. P., and McInnes, K. J.: Pathways of dye tracer movement through structured soils on a macroscopic scale, Soil Sci., 169, 229–242, 2004. 11042, 11043

Noguchi, S., Tsuboyama, Y., Sidle, R. C., and Hosoda, I.: Morphological characteristics of macropores and the distribution of preferential flow pathways in a forested slope segment, Soil Sci. Soc. Am. J., 63, 1413–1423, 1999. 11042, 11043

Pierson, T. C.: Soil pipes and slope stability, Q. J. Eng. Geol., 16, 1–15, 1983. 11042

Sidle, R. C., Tsuboyama, Y., Noguchi, S., Hosada, I., Fujieda, M., and Shimizu, T.: Stormflow generation in steep forested headwaters: a linked hydrogeomorphic paradigm, Hydrol. Process., 14, 369–385, 2000. 11043, 11050

Sidle, R. C., Noguchi, S., Tsuboyama, Y., and Laursen, K.: A conceptual model of preferential flow systems in forested hillslopes: evidence of self-organization, Hydrol. Process., 15, 1675–1692, doi:10.1002/hyp.233, 2001. 11043

Tsuboyama, Y., Sidle, R. C., Noguchi, S., and Hosada I.: Flow and transport through the soil matrix and macropores of hillslope segment, Water Resour. Res., 30, 879–890, 1994. 11042, 11043, 11050

Trojan, M. and Linden, D.: Micro relief and rainfall effects on water and solute movement in eartchworm burrows, Soil Sci. Soc. Am. J., 56, 727–733, 1992. 11042

Uchida, T., Kosugi, K., and Mizuyama, T.: Effects of pipeflow on hydrological process and its relation to landslide: a review of pipeflow studies in forested headwater catchments, Hydrol. Process., 15, 2151–2174, 2001. 11042

Weiler, M. and McDonnell, J. J.: Conceptualizing lateral preferential flow and flow networks and simulating the effects on gauged and ungauged hillslopes, Water Resour. Res., 43, W03403, doi:10.1029/2006WR004867, 2007. 11044

Weiler, M. and Naef, F.: An experimental tracer study of the role of macropores in infiltration in grassland soils, Hydrol. Process., 17, 477–493, 2003. 11042, 11043

Wu, W. and Sidle, R. C.: A distributed slope stability model for steep forested basins, Water Resour. Res., 31, 2097–2110, 1995. 11044

Van Asch, Th. W. J., Hendriks, M. R., Hessel, R., and Rappange, F. E.: Hydrological triggering conditions of landslides in varved clays in the French Alps, Eng. Geol., 42, 239–251, 1996. 11042

Van Asch, Th. W. J., van Dijk, S. J. E., and Hendriks, M. R.: The role of overland flow and subsurface flow on the spatial distribution of soil moisture in the topsoil, Hydrol. Process., 15, 2325–2340, 2001. 11041

Van Asch, Th. W. J., Van Beek L. P. H., and Bogaard, T. A.: Problems in predicting the mobility of slow-moving landslides, Eng. Geol., 91, 46–55, 2007. 11041

Van Beek, L. P. H.: Assessment of the influence of changes in land use and climate on landslide activity in a Mediterranean environment, PhD Thesis, University of Utrecht, The Netherlands, 2002. 11042, 11045, 11047, 11056, 11058, 11064, 11065

Van Beek, L. P. H. and van Asch, T. W. J.: A combined conceptual model for the effects of fissure-induced infiltration on slope stability, In Process Modelling and Landform Evolution, Lect. Notes Earth Sci., 78, 147–167, doi:10.1007/BFb0009716, 1999. 11042, 11044, 11045, 11046

Van Schaik, L.: The role of macropore flow, from plot to catchment scale. A study in a semi-arid area, PhD Thesis, University of Utrecht, The Netherlands, 2010. 11043, 11044

Van Westen, C. J., van Asch, T. W. J., and Soeters R.: Landslide hazard and risk zonation: why it is so difficult?, B. Eng. Geol. Envir., 65, 167–184, 2005. 11044

Zehe, E. and Bloschl, G.: Predictability of hydrologic response at the plot and catchment scales – the role of initial conditions, Water Resour. Res., 40, W10202, doi:10.1029/2003WR002869, 2004 11044, 11050

Zhang, G. P., Savenije, H. H. G., Fenicia, F., and Pfister, L.: Modelling subsurface storm flow with the Representative Elementary Watershed (REW) approach: application to the Alzette River Basin, Hydrol. Earth Syst. Sci., 10, 937–955, doi:10.5194/hess-10-937-2006, 2006. 11044

HESSD
8, 11039–11073, 2011



D. M. Krzeminska et al.





**Table 1.** Annual water balance components of four modelled scenarios.

| | No fissures | Disconnected fissures | Connected fissures | Dynamic connectivity |
|---|---|---|---|---|
| Total storage at the start of simulated period [$m^3$] | 57618 | 62571 | 62571 | 62571 |
| Total rain input [$m^3\,yr^{-1}$] | 61681 | 61681 | 61681 | 61681 |
| Total storage at the end of simulated period [$m^3$] | 57431 | 62595 | 60432 | 61677 |
| Change in total storage over the simulation period [$m^3$] | -187 | 24 | -2139 | -894 |
| Total outflow [$m^3\,yr^{-1}$] | 21933 | 21685 | 23256 | 22623 |
| Total evaporation [$m^3\,yr^{-1}$] | 39927 | 39961 | 40555 | 39944 |

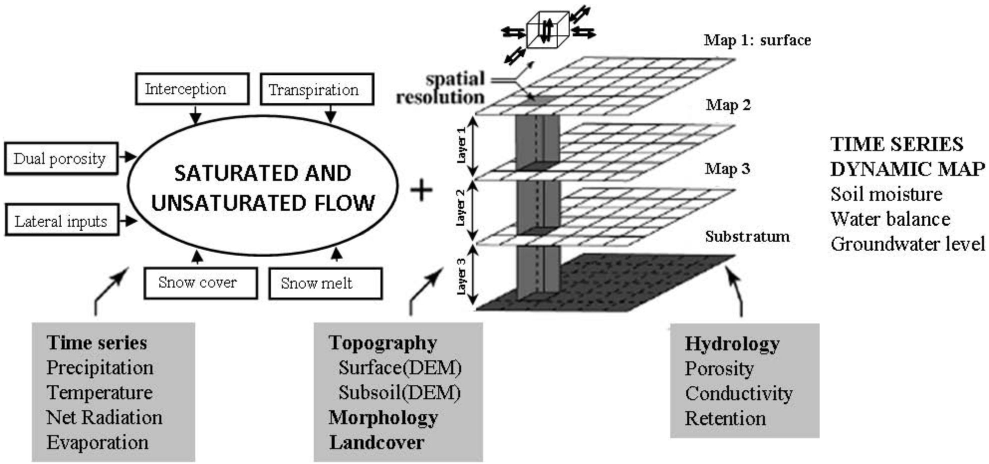


**Fig. 1.** Architecture of STARWARS model (core model and sub-models) and schematic representation of the model implementation (adopted from Malet et al., 2005, based on Van Beek, 2002).





HESSD
8, 11039–11073, 2011

Influence of fissures on landslide activity

D. M. Krzeminska et al.

Title Page
Abstract | Introduction
Conclusions | References
Tables | Figures
◀I | ▶I
◀ | ▶
Back | Close
Full Screen / Esc
Printer-friendly Version
Interactive Discussion

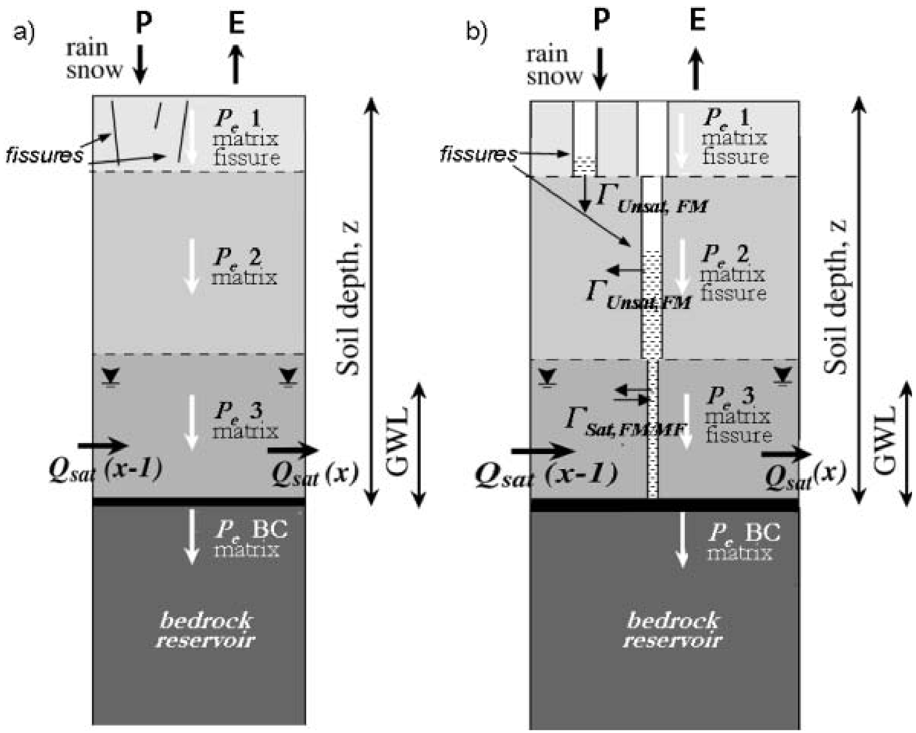


**Fig. 2.** Schematisation of **(a)** the original hydrological model (after Van Beek, 2002 Malet et al., 2005) and **(b)** the hydrological model implemented with this research.

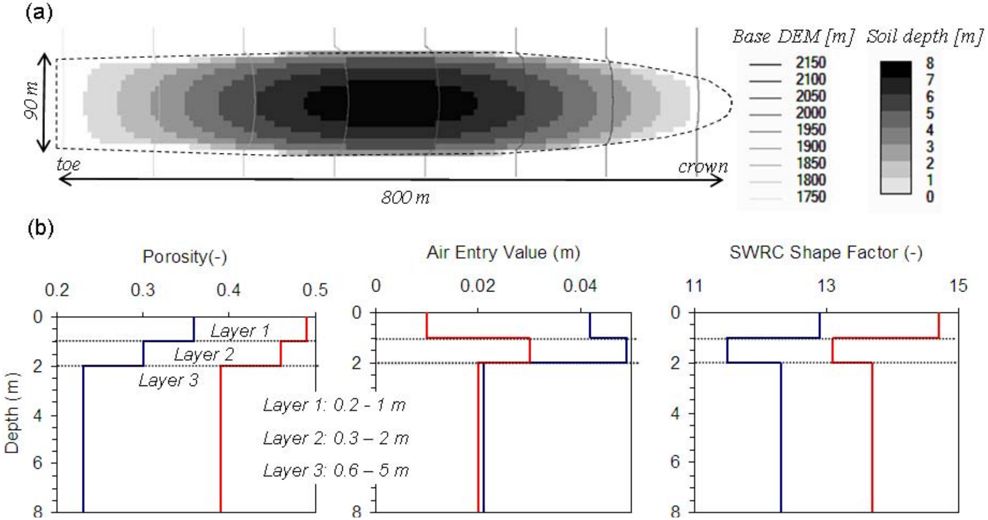


**Fig. 3.** **(a)** Geometry of the idealised, "simple" landslide representation, **(b)** hydrological parameters of the soil layers; blue are matrix fraction characteristics and red lines fissures fraction characteristics.





HESSD
8, 11039–11073, 2011

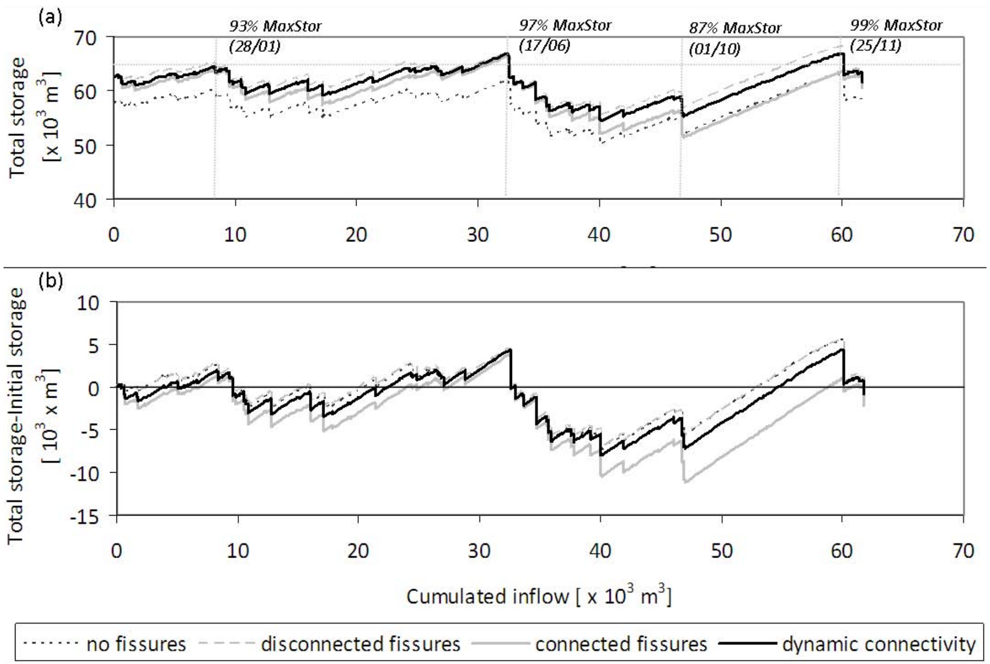


**Fig. 4.** Variation in total storage during one-year simulation period expressed as a relationship between **(a)** total storage and **(b)** changes in total storage compared to initial condition and cumulated inflow (total rain volume).





HESSD
8, 11039–11073, 2011

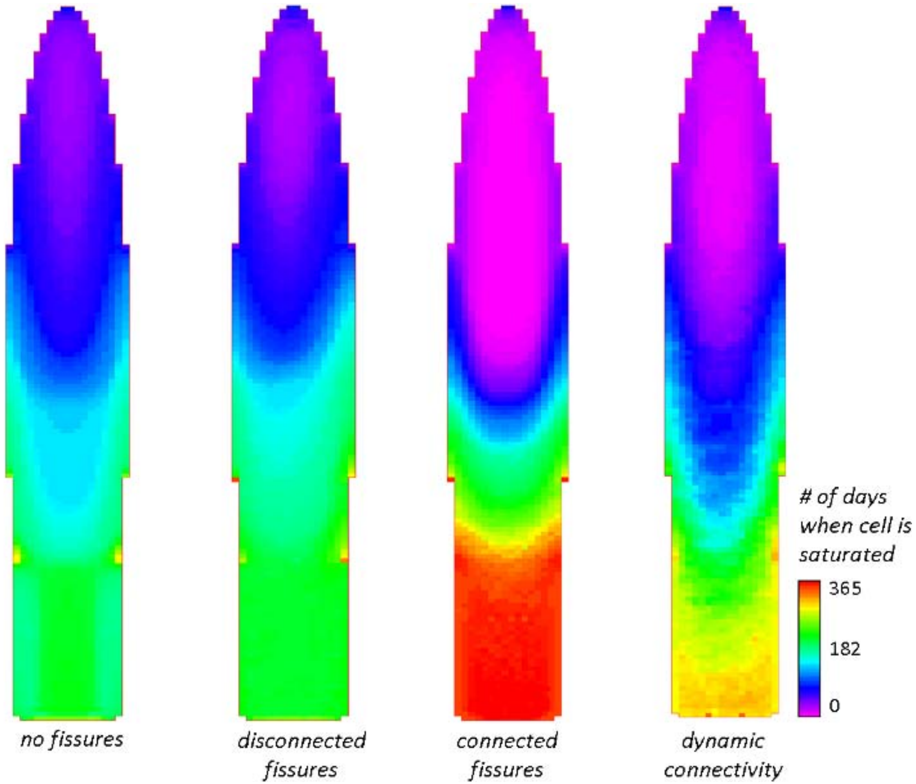


**Fig. 5.** The total number of days during one year simulation period that full saturation was observed.





HESSD
8, 11039–11073, 2011

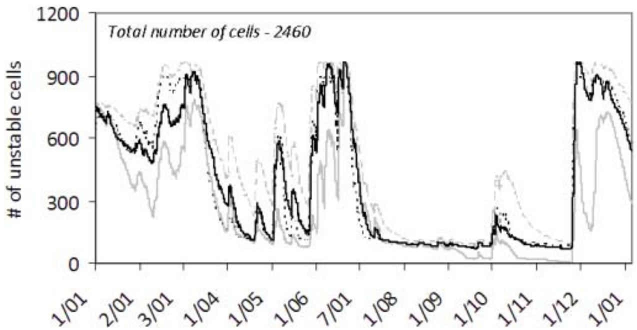


| | Average* | Min* | Max* |
|---|---|---|---|
| no fissures | 15.6% | 3.0% | 36.2% |
| disconnected | 20.4% | 3.5% | 39.0% |
| connected | 11.2% | <0.5% | 39.0% |
| dynamic | 16.0% | 2.8% | 39.0% |

** % of total number of cells*

**Fig. 6.** The number of unstable cells ($f_s < 1$) per time step, observed with different scenarios.





HESSD
8, 11039–11073, 2011

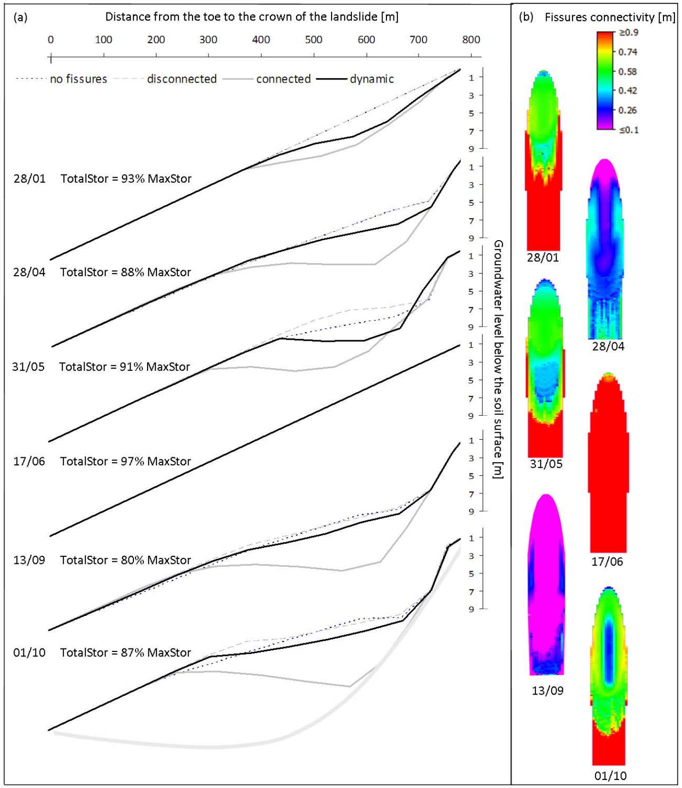


**Fig. 7. (a)** Modelled groundwater levels along the landslide profile (major axes of the ellipse); x-axis represents the distance from the toe of the landslide (0 m) to the crown (800 m). The light grey line present at the last profile represents the bedrock depth. **(b)** The distribution of fissures connectivity over the landslide area, corresponding to these groundwater levels and storage capacities.





HESSD
8, 11039–11073, 2011

Influence of fissures on landslide activity

D. M. Krzeminska et al.

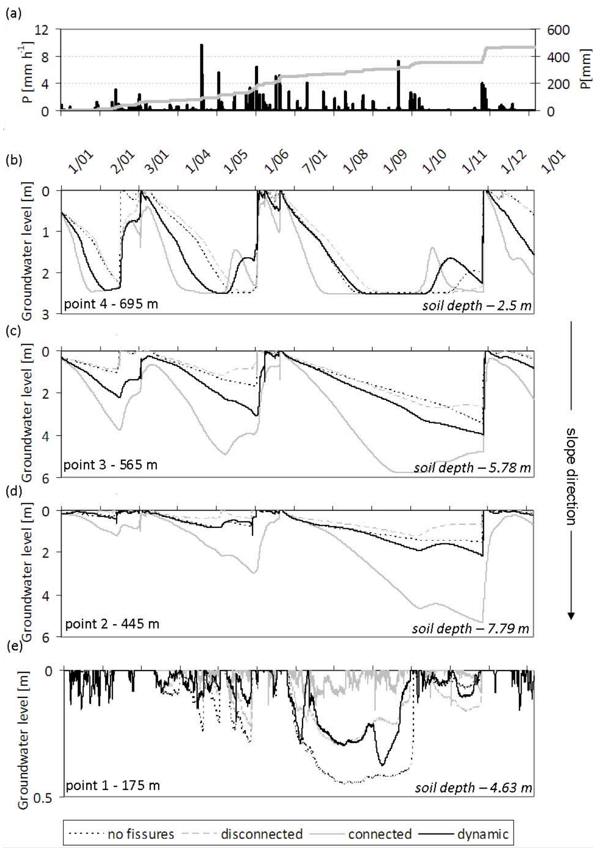


**Fig. 8.** Time series results of the 1 yr simulation period. **(a)** Precipitation, **(b–e)** examples of groundwater level fluctuations observed in four points located along the landslide profile (major axes of the ellipse) from the toe (0 m) to the scarp (800 m) of the landslide. See Fig. 7a for the landslide profile.





HESSD
8, 11039–11073, 2011

Influence of fissures on landslide activity

D. M. Krzeminska et al.

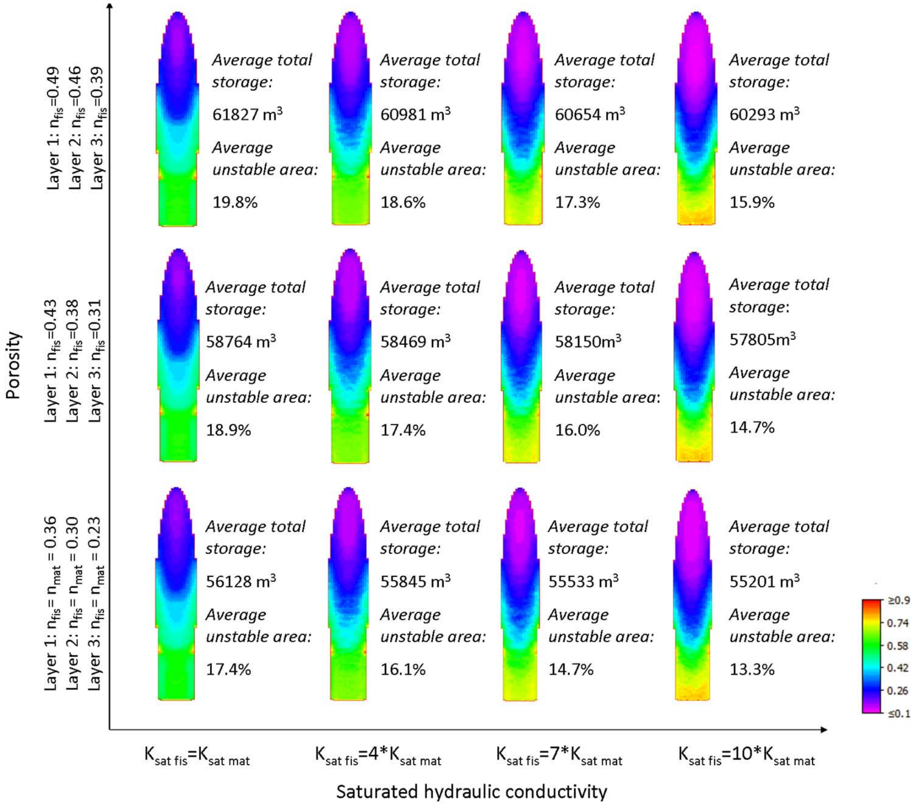


**Fig. 9.** Sensitivity analysis of the model for changes in the fissure parameterisation. The unstable area is the area of all cells with $f_s < 1$.





HESSD
8, 11039–11073, 2011

**Influence of fissures on landslide activity**

D. M. Krzeminska et al.

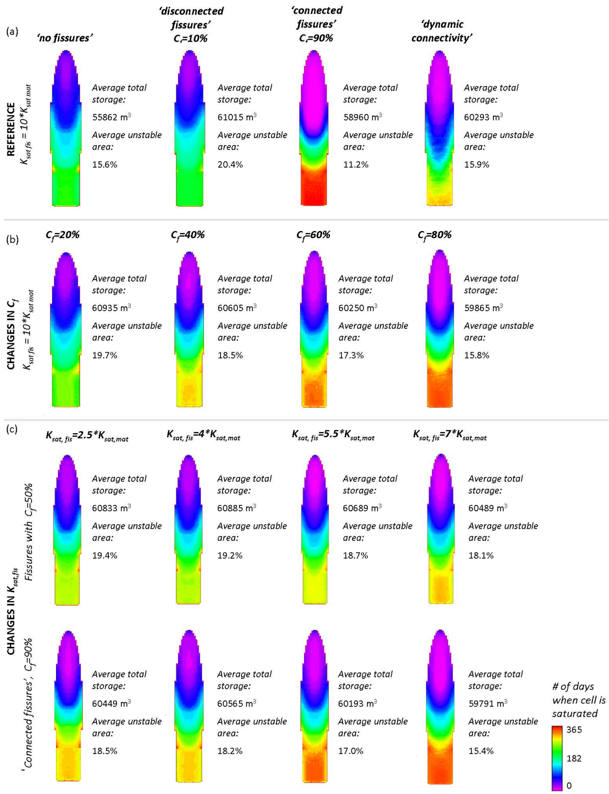


**Fig. 10.** Sensitivity analysis of the model for changes in conceptualisation of fissure connectivity: **(a)** is the reference panel - the "no fissure", "disconnected fissures", "connected fissures" and "dynamic connectivity" scenarios; **(b)** changing fissure connectivity ($C_{fis}$) for the simulation with fissures included ($C_{fis}$ is constant over the simulation period); **(c)** changing saturated hydraulic conductivity for the "disconnected fissure" and 'connected fissures' scenario The unstable area is the area of all cells with $f_s < 1$.





HESSD
8, 11039–11073, 2011



Title Page
Abstract | Introduction
Conclusions | References
Tables | Figures
◀| |▶
◀ ▶
Back | Close
Full Screen / Esc
Printer-friendly Version
Interactive Discussion